Reaction dynamics and nuclear structure of moderately neutron-rich Ne isotopes by heavy-ion reactions

S. Bottoni,[1,2] G. Benzoni,[2] S. Leoni,[1,2,*] D. Montanari,[1,2,†] A. Bracco,[1,2] F. Azaiez,[3] S. Franchoo,[3] I. Stefan,[3] N. Blasi,[2] F. Camera,[1,2] F. C. L. Crespi,[1,2] A. Corsi,[1,2] B. Million,[2] R. Nicolini,[1,2] E. Vigezzi,[2] O. Wieland,[2] F. Zocca,[1,2] L. Corradi,[4] G. De Angelis,[4] E. Fioretto,[4] B. Guiot,[4] N. Marginean,[4,5] D. R. Napoli,[4] R. Orlandi,[4] E. Sahin,[4] A. M. Stefanini,[4] J. J. Valiente-Dobon,[4] S. Aydin,[6] D. Bazzacco,[6] E. Farnea,[6] S. Lenzi,[6,7] S. Lunardi,[6,7] P. Mason,[6,7] D. Mengoni,[7] G. Montagnoli,[6,7] F. Recchia,[6,7] C. Ur,[6] F. Scarlassara,[6,7] A. Gadea,[8] A. Maj,[9] J. Wrzesinski,[9] K. Zuber,[9] Zs. Dombradi,[10] S. Szilner,[11] A. Saltarelli,[12] and G. Pollarolo[13]

[1]*Dipartimento di Fisica, University of Milano, Milano, Italy*
[2]*INFN, Sezione di Milano, Milano, Italy*
[3]*IPN, Orsay, France*
[4]*INFN Laboratori Nazionali di Legnaro, Padova, Italy*
[5]*National Institute of Physics and Nuclear Engineering, Bucharest-Magurele, Romania*
[6]*INFN, Sezione di Padova, Padova, Italy*
[7]*Dipartimento di Fisica, University of Padova, Padova, Italy*
[8]*CSIC-IFIC, Valencia, Spain*
[9]*Niewodniczanski Institute of Nuclear Physics, Polish Academy of Sciences, Krakow, Poland*
[10]*Atomki, Debrecen, Hungary*
[11]*Ruđer Bošković Institute, Zagreb, Croatia*
[12]*University of Camerino and INFN, Sezione di Perugia, Perugia, Italy*
[13]*Dipartimento di Fisica Teorica, University of Torino, and INFN, Sezione di Torino, Torino, Italy*

(Received 8 May 2012; published 28 June 2012)

The heavy-ion reaction ^{22}Ne + ^{208}Pb at 128 MeV beam energy has been studied using the PRISMA-CLARA experimental setup at Legnaro National Laboratories. Elastic, inelastic, and one-nucleon transfer differential cross sections are measured and global agreement is obtained with semiclassical and distorted-wave Born approximation (DWBA) calculations. In particular, the angular distribution of the 2^+ state of ^{22}Ne is analyzed by DWBA and a similar calculation is performed for the unstable ^{24}Ne nucleus, using existing data from the reaction ^{24}Ne + ^{208}Pb at 182 MeV (measured at SPIRAL with the VAMOS-EXOGAM setup). In both cases the DWBA model gives a good reproduction of the experiment, pointing to a strong reduction of the β_2^C charge deformation parameter in ^{24}Ne. This follows the trend predicted for the evolution of the quadrupole deformation along the Ne isotopic chain.

DOI: 10.1103/PhysRevC.85.064621 PACS number(s): 25.70.Bc, 25.70.Hi, 24.10.Eq, 27.30.+t

I. INTRODUCTION

Low-energy transfer reactions with heavy ions have recently become a powerful tool for the production and investigation of exotic neutron-rich systems not accessible by standard fusion evaporation reactions [1,2]. In particular, the combination of a large acceptance magnetic spectrometer with a high efficiency and high resolution multidetector array for γ spectroscopy (based on Ge detectors) has turned out to be a key instrument in linking reaction dynamics and nuclear structure studies far from stability [3,4]. Recent work, focusing on nuclei in the mass region around doubly magic ^{48}Ca, have clearly demonstrated the possibility of employing heavy-ion transfer reactions both for detailed particle-spectroscopy (with enhanced sensitivity to specific excited states by γ-gating techniques) and to perform full in-beam γ spectroscopy (i.e., angular distributions, polarizations, and lifetime analysis) [5–7]. That work has outlined a new method which can become very valuable for future investigations, also in the case of radioactive heavy-ion beams, providing complementary information to transfer reactions with light targets.

In this paper, we discuss the results of a similar analysis on light neutron-rich nuclei around ^{22}Ne, which are instrumental for the understanding of the evolution of the shell structure moving towards the neutron drip line. This is the region close to the so-called island of inversion, where a weakening of the $N = 20$ magic number has been observed. In particular, we present the study of the dynamics of the heavy-ion binary reaction ^{22}Ne + ^{208}Pb (at 128 MeV), performed at Legnaro National Laboratories with the PRISMA-CLARA setup, allowing for particle-γ coincidence experiments. The analysis focuses on the measurement of differential cross sections for the elastic, inelastic, and one-particle transfer channels. The experimental data are interpreted by the semiclassical model GRAZING [8] and by the distorted-wave Born approximation approach (DWBA), implemented in the code PTOLEMY [9]. The latter can be used to obtain information on the parameters of the optical model potential, which are directly connected to the structure and deformation of the colliding nuclei. In the case of the inelastic scattering to the 2^+ state of ^{22}Ne,

*Corresponding author: silvia.leoni@mi.infn.it
†Present address: University of Padova, Padova, Italy.

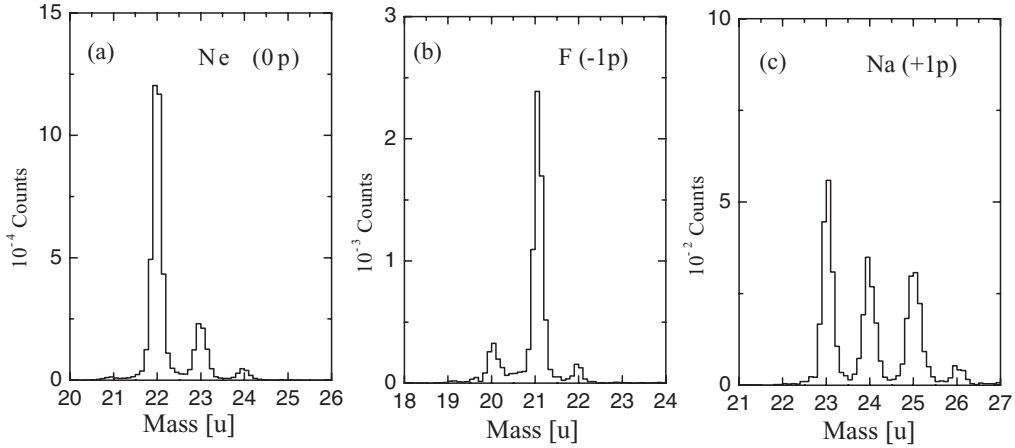

FIG. 1. Mass spectra of the most intense isotopic chains produced in the ^{22}Ne + ^{208}Pb reaction. (a) Pure neutron transfer, (b) one-proton stripping, and (c) one-proton pickup reaction channels.

the present results are also compared with existing data from the reaction ^{24}Ne + ^{208}Pb (at 182 MeV), obtained in a similar experiment at GANIL using the VAMOS-EXOGAM setup, starting from the radioactive ^{24}Ne beam from SPIRAL [10]. In both cases, a DWBA analysis is performed and β_2^C deformation parameters for the nuclear charge distributions are extracted and compared to existing experimental values and to predictions of the evolution of the quadrupole deformation along the Ne isotopic chain. The results follow the trend predicted by various calculations, supporting the existence of a deformation minimum at ^{24}Ne ($N = 14$).

The paper is organized as follows. In Sec. II we describe the ^{22}Ne + ^{208}Pb reaction and the experimental setup, briefly recalling the procedure adopted for the identification of the reaction products in the magnetic spectrometer. In Sec. III we discuss the main points of the analysis, which focuses on the study of the elastic, inelastic, and one-nucleon transfer channels. Emphasis is given to the inelastic scattering data and their interpretation by the DWBA model. Conclusions are given in Sec. IV.

II. EXPERIMENT

The experiment was performed at the Legnaro National Laboratories of INFN, using the PRISMA-CLARA experimental setup [11]. The ^{22}Ne beam, provided by the PIAVE-ALPI accelerator complex at 128 MeV of bombarding energy, impinged on a ^{208}Pb target 300 μg/cm^2 thick, sandwiched between two layers of ^{12}C (10 and 15 μg/cm^2 thick respectively). The magnetic spectrometer PRISMA, described in Refs. [12–15], was placed around the grazing angle for this reaction, which has been estimated to be $\theta_{\rm lab} = 70^\circ$. PRISMA consists of one quadrupole and one dipole magnet, with a solid angle of 80 msr (corresponding to $\pm 6^\circ$ in θ and $\pm 13^\circ$ in ϕ), a momentum acceptance $\Delta p/p = 10\%$, and a dispersion of 4 cm per percent in momentum. Being based on a system of entrance and focal plane detectors (consisting of a microchannel plate detector and an ionization chamber plus an array of parallel plates of multiwire type, respectively), the trajectory of the ions in the PRISMA spectrometer can be reconstructed, event by event. As described in detail in Ref. [5], the identification of the reaction products is achieved (i) by determining the atomic number Z through the energy released in the ionization chamber and (ii) by determining the A/q ratio via time-of-flight and ion trajectory measurements for each charge state q. The coupling of the PRISMA spectrometer with the γ-array CLARA, placed opposite to PRISMA, made possible particle-γ coincidence measurements for each ion detected in the magnetic spectrometer. In the present experiment, the CLARA array consisted of 21 high-purity germanium (HPGe) clover detectors covering a solid angle of 2π, with a total efficiency of the order of 2.5% at 1.3 MeV.

Figure 1 shows the mass spectra for the most intense products populated in the ^{22}Ne + ^{208}Pb experiment. They correspond to pure neutron transfer ($0p$), one-proton stripping ($-1p$) and one-proton pickup ($+1p$) reaction channels. As already observed in a similar work on heavier systems around ^{48}Ca [5], a slight asymmetry is visible in the one-proton transfer products, pointing to a favorable population of lighter (heavier) masses in the stripping (pickup) channels.

III. ANALYSIS

The aim of the present work is the evaluation of absolute differential cross sections for elastic, inelastic and one-particle transfer channels. For this purpose, the response function of PRISMA for the specific ^{22}Ne + ^{208}Pb reaction had to be determined by the Monte Carlo procedure described in Ref. [15]. This is needed for a correct treatment of the measured yields, which can be strongly affected by the transmission into the spectrometer, especially at the edges of the angular acceptance. As a second point, the elastic channel was studied in detail in order to provide both a reference scale for cross-section measurements and the starting point for a reaction dynamics investigation.

Following the method described in Ref. [16] and successfully applied in previous works [5,10,16], total kinetic energy loss spectra (TKEL), defined as TKEL $= -Q_{\rm value}$, were constructed, as a function of the scattering angle, for the ^{22}Ne ions detected in PRISMA. They were used to obtain

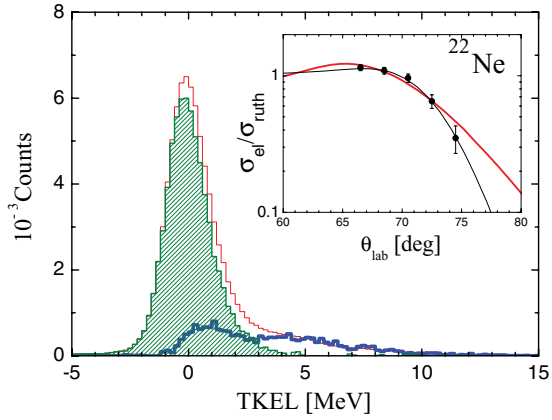

FIG. 2. (Color online) TKEL spectra for ^{22}Ne ions detected by PRISMA (thin red line) and in coincidence with γ transitions detected in CLARA (thick blue line). The shaded area is the difference spectrum corresponding to elastic events. Inset: Elastic cross section over Rutherford cross section as a function of the scattering angle. The experimental data (circles) have been normalized in the Rutherford region to the theoretical calculation performed by the code GRAZING (thin black line). The calculation performed by the PTOLEMY code (with the optical model parameters listed in Table I) is shown by the thick red line.

the elastic cross section by subtracting TKEL spectra of ^{22}Ne measured in coincidence with γ transitions detected in the CLARA array. The latter represent the inelastic contribution to the TKEL distributions. Due to the different efficiencies of the PRISMA and CLARA setups, this subtraction can be performed only after a proper normalization of the two spectra. This is done in the high excitation energy region (above 4 MeV) where the total and inelastic TKEL spectra must coincide, as shown in Fig. 2. The difference spectrum (shaded area) is a peak centered at TKEL $\approx$0, with a FWHM of $\approx$2.5 MeV, which agrees with t he energy resolution of the experimental setup. It consists of elastic events, whose ratio with the Rutherford cross section, over the angular acceptance of the magnetic spectrometer ($64^\circ \leqslant \theta_{lab} \leqslant 76^\circ$), is shown in the inset of Fig. 2. The experimental data have been normalized, in the pure Rutherford region ($\theta_{lab} = 66.5^\circ$), to the theoretical ratio $\sigma_{el}/\sigma_{Ruth}$, calculated by the semiclassical code GRAZING [8]. This allows us to both extract a conversion factor between counts and mb/sr (i.e., 1 mb/sr = 215 counts) and confirm the validity of the experimental procedure. To further check this experimental result, a more detailed study of the elastic cross section was done with the DWBA model implemented

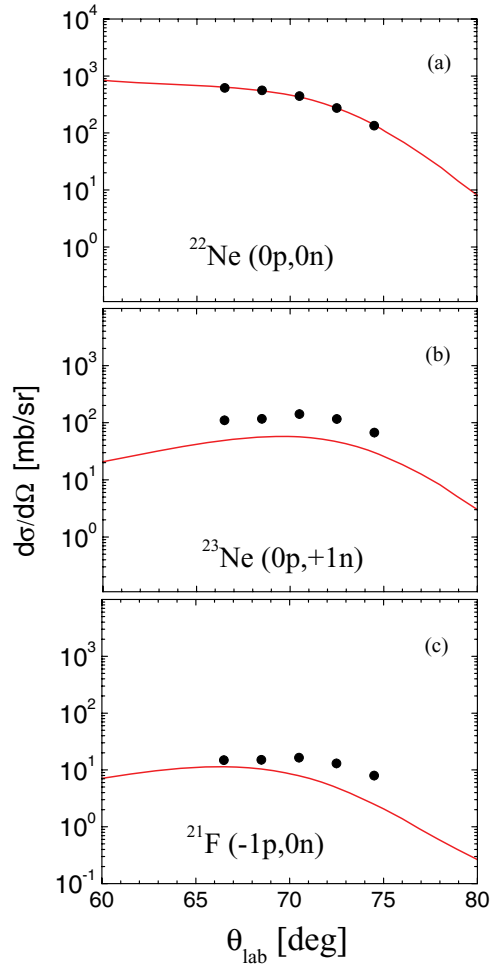

FIG. 3. (Color online) Inclusive angular distributions for the most intense reaction channels ^{22}Ne, ^{23}Ne, and ^{21}F. Symbols correspond to experimental data, solid lines to theoretical calculations by the semiclassical model GRAZING [8].

in the PTOLEMY code [9]. The parameters used for the nuclear potential, reported in Table I, were obtained by fitting the $\sigma_{el}/\sigma_{Ruth}$ experimental data and are consistent with the values used by the GRAZING model (see the discussion of inelastic scattering for a detailed description of the parameters). The result of the PTOLEMY calculation is shown in the inset of Fig. 2 by the thick solid line.

The extracted conversion factor between counts and mb/sr WAS kept as a reference for the following analysis of differential cross sections. Figure 3 shows the inclusive (energy

TABLE I. Parameters of the Wood-Saxon optical potentials describing the collisions ^{22}Ne + ^{208}Pb at 128 MeV and ^{24}Ne + ^{208}Pb at 182 MeV. V and W indicate the depth of the real and imaginary parts, a_V and a_W the corresponding diffusenesses. r_V and r_W are the radii of the real and imaginary potential, while r_C is the radius of the Coulomb potential, for which standard values are used. The β_2 deformation parameters were obtained by fitting the inelastic cross section. It is assumed $\beta_2 = \beta_2^C = \beta_2^N$. (See text for details.)

	V (MeV)	r_V (fm)	a_V (fm)	W (MeV)	r_W (fm)	a_W (fm)	r_C (fm)	β_2
^{22}Ne	67.37	1.167	0.668	19.26	1.167	0.668	1.25	0.370
^{24}Ne	66.98	1.167	0.671	35.00	1.167	0.671	1.25	0.075

integrated) angular distribution for the elastic channel [^{22}Ne in Fig. 1(a)], the one neutron pickup channel [^{23}Ne in Fig. 1(b)], and the one-proton stripping channel [^{21}F in Fig. 1(c)], which are the most intense reaction products. The experimental data are compared with theoretical calculations performed by the semiclassical GRAZING model, which is able, in general, to well describe one-particle transfer processes in low-energy heavy-ion binary reactions [1,8]. We see that the experimental angular distributions are rather well reproduced by the calculations, with a global agreement between data and theory. Similar quality of agreement was also obtained for the one-nucleon transfer channels in the work of Ref. [10], where the more exotic ^{25}Ne and ^{23}F channels were studied, following the heavy-ion reaction ^{24}Ne + ^{208}Pb. This indicates that the basic ingredients entering the prescription of the reaction dynamics by the GRAZING model are still valid in the case of heavy-ion reactions induced by rather light systems such as Ne isotopes, and moving away from the stability valley.

The γ spectra measured by the CLARA array in coincidence with the most intense ^{22}Ne, ^{23}Ne, and ^{21}F channels are shown in Fig. 4. They have been Doppler corrected, on an event-by-event basis, using the velocity and angles provided by the trajectory reconstruction in the PRISMA spectrometer. In all three cases, the decay from the first excited state is clearly observed. Moreover, in the case of ^{22}Ne, the $2^+ \rightarrow 0^+$ transition at 1275 keV has enough statistics to determine the differential cross section for the inelastic scattering to the 2^+ state. This has been done by integrating the area of the 1275 keV peak for each $\theta_{\rm lab}$ angle covered by the acceptance of PRISMA. As reported in Ref. [5], this procedure provides the direct population of the first excited state, after

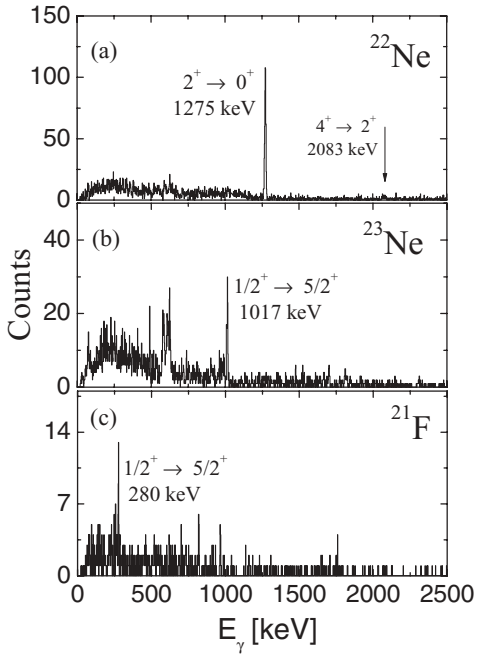

FIG. 4. γ spectra of ^{22}Ne, ^{23}Ne, and ^{21}F. In each spectrum the γ transition from the first excited state to the ground state is clearly visible. For ^{22}Ne, the arrow indicates the position of the $4^+ \rightarrow 2^+$ decay, at 2083 keV, not observed in this experiment.

subtracting the feeding contribution from higher lying levels and taking into account the γ efficiency of the CLARA array. In this case, the feeding from the $4^+ \rightarrow 2^+$ decay is negligible, as indicated by the absence of the corresponding γ peak in Fig. 4(a), while at most a 25% feeding contribution can be expected from higher lying states around 5 MeV. This is suggested by the presence of a high-energy tail in the TKEL spectrum gated by the $2^+ \rightarrow 0^+$ γ transition, as shown in the inset of Fig. 5(a). In the same panel, the results (open symbols) are presented together with the data corrected for this feeding contribution (filled circles). In Fig. 5(b) we present inelastic scattering data taken from Ref. [10], relative to the 2^+ state of the unstable ^{24}Ne, populated by the ^{24}Ne + ^{208}Pb reaction at 182 MeV.

Calculations of the inelastic scattering to the 2^+ state were performed for both experiments, using the DWBA model, implemented in the code PTOLEMY [9]. For the Woods-Saxon optical model potentials we used the parameters reported

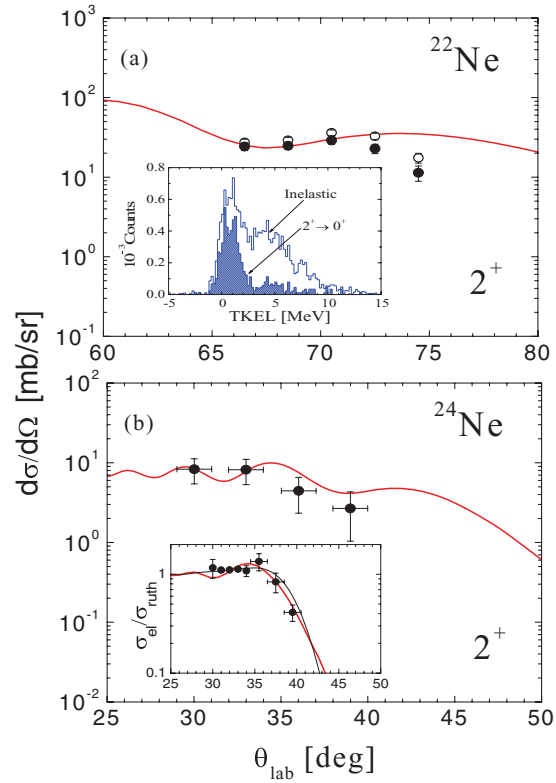

FIG. 5. (Color online) (a) Angular distribution of ^{22}Ne ions measured in coincidence with the $2^+ \rightarrow 0^+ \gamma$ transition of 1275 keV. Filled (open) symbols refer to the analysis performed on the γ spectrum of ^{22}Ne taking (not taking) into account the feeding from high-lying states around 5 MeV. Inset of (a): inelastic TKEL spectrum of ^{22}Ne and the contribution coming from the $2^+ \rightarrow 0^+$ γ decay (shaded area). (b) Angular distribution of ^{24}Ne, measured in coincidence with the $2^+ \rightarrow 0^+$ γ transition of 1982 keV. Inset of panel (b): elastic over the Rutherford cross section of ^{24}Ne, as a function of the scattering angle. Experimental data are indicated by symbols, while theoretical calculations performed by the code PTOLEMY (GRAZING) are given by thick red (thin black) lines. Data for ^{24}Ne are taken from Ref. [10]. (See text for details.)

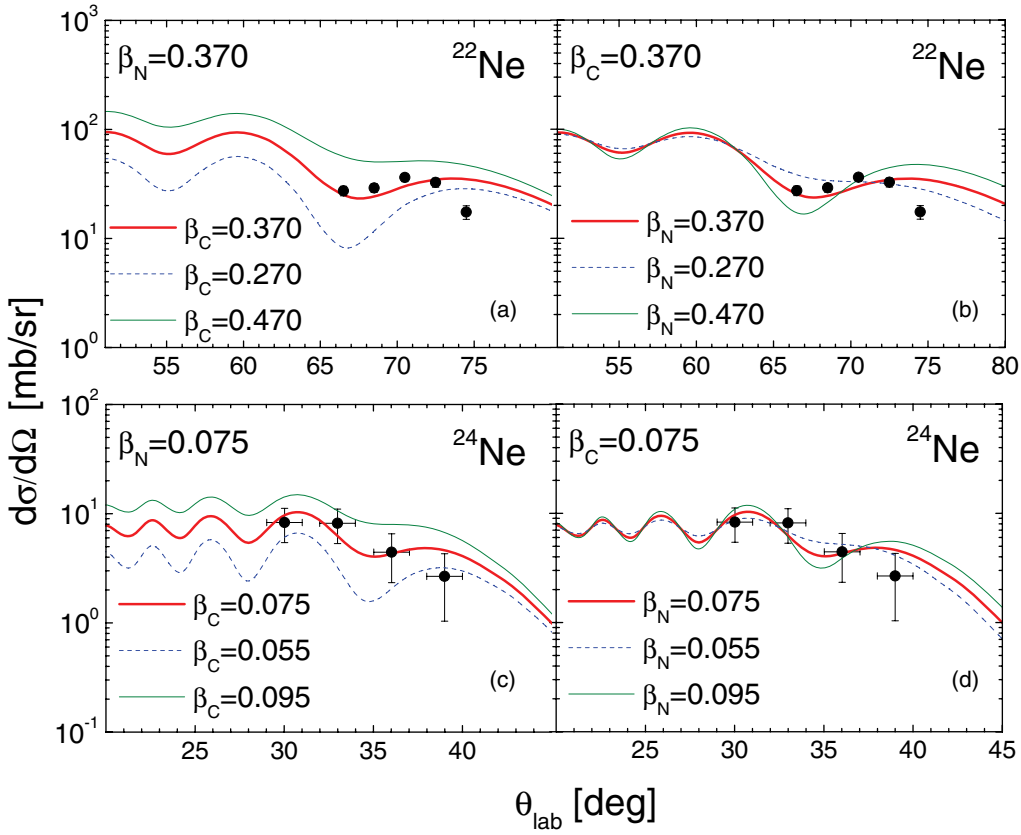

FIG. 6. (Color online) Angular distributions of ^{22}Ne and ^{24}Ne measured in coincidence with the corresponding $2^+ \rightarrow 0^+$ transitions. Symbols refer to data, lines to DWBA calculations performed by the PTOLEMY code, assuming different values for the parameters β_2^C and β_2^N, as given in the legends. (See text for details.)

in Table I. In particular, the depth V and the diffuseness a_V of the real part were taken from the proximity potential model [17], while the real radius r_V and the imaginary depth W were determined by the fit of the $\sigma_{\rm el}/\sigma_{\rm Ruth}$ experimental data [see Fig. 2 and the inset of Fig. 5(b) for ^{24}Ne]. The assumption $r_W = r_V$ and $a_W = a_V$ was adopted for the radius and diffuseness of the imaginary part of the nuclear potential. Furthermore, we have put $\beta_2^C = \beta_2^N$, because the fit to the inelastic cross sections favored very similar values for the nuclear and Coulomb deformation parameters. This is shown in Fig. 6, where the sensitivity to the deformation parameters β_2^C and β_2^N is investigated for both ^{22}Ne and ^{24}Ne by changing the optimal β_2^C and β_2^N values by 25%. In particular, we note that the fit of the inelastic distribution is not very sensitive to the value of β_2^N, while the variation of β_2^C influences the strength of the inelastic cross sections in a similar way for both nuclei. As a consequence, in the following we discuss our results only in terms of charge deformation parameters β_2^C.

The values for β_2^C obtained by the experimental analysis of ^{22}Ne and ^{24}Ne are reported in the last column of Table I and in Fig. 7(a) by filled diamonds. It is found that ^{22}Ne has a rather large quadrupole deformation ($\beta_2^C \approx 0.4$), with a value consistent with the one obtained by an earlier analysis of ^{22}Ne + ^{208}Pb inelastic-scattering data, performed with a rotational coupled-channel model [18]. In that work the reaction ^{22}Ne + ^{208}Pb was also studied, and a very similar value was obtained for ^{20}Ne (following the ^{20}Ne + ^{208}Pb reaction), as shown by open diamonds in Fig. 7(a). On the contrary, in the present analysis small values for the deformation parameters of ^{24}Ne are found ($\beta_2^C \approx 0.1$).

It is interesting to compare our β_2^C values with the charge deformation parameters derived from experimental $B(E2; 0^+ \rightarrow 2^+)$ measurements (Coulomb excitation or lifetime analysis techniques). Such values can be obtained, for example, by the droplet model of Ref. [19], or by applying the first-order formula

$$\beta_2^C = \left(4\pi/3ZR_0^2\right)[B(E2; 0^+ \rightarrow 2^+)/e^2]^{1/2}, \qquad (1)$$

with $R_0 = 1.2A^{1/3}$ the spherical radius of the nuclear charge distribution. In Fig. 7(a) we show by open circles the "adopted" β_2^C values [20], while filled circles refer to the most recent measurements derived from intermediate energy Coulomb excitation experiments (at MSU and RIKEN) and from low-energy Coulomb excitation measurements (at ISOLDE) [21–24]. These recent values are systematically lower than the adopted ones, clearly indicating the difficulty in determining experimentally a firm value for the β_2^C parameter. Our results are also significantly smaller than the adopted value. They

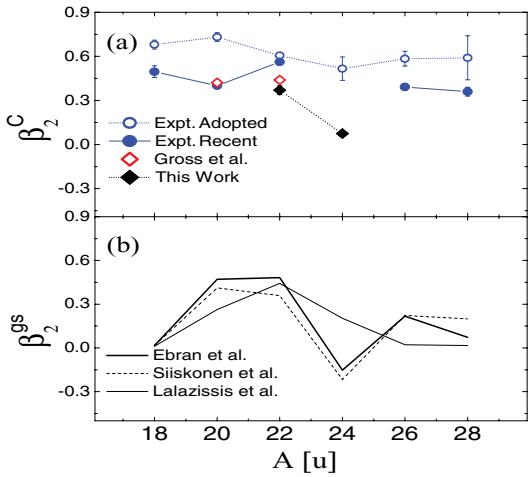

FIG. 7. (Color online) (a) Quadrupole deformation parameter β_2^C of the nuclear charge distribution, along the isotopic Ne chain, as derived from experiments. Filled diamonds refer to this work, open diamonds to a similar analysis performed by Gross *et al.* [18], open circles to the experimental adopted values [20], filled circles to the most recent results from Coulomb excitation experiments [21–24]. (b) Theoretical predictions for the ground state deformation parameter $\beta_2^{\rm gs}$, as indicated by the legend [26–28]. (See text for details.)

correspond to a 30% reduction in the case of ^{22}Ne (which could be accounted for by the uncertainty of the different experimental techniques) and to a much larger suppression (of the order of a factor of 5) for ^{24}Ne. In this case, the adopted value corresponds to the only existing $B(E2)$ measurement via the lifetime technique, reported in Ref. [25]. Such a large discrepancy is rather puzzling and definitely calls for additional experimental investigation on the collectivity in ^{24}Ne, a nucleus of key importance for understanding the evolution of shell gaps in light systems, moving towards the neutron drip line.

In Fig. 7(b) we show the deformation parameters of the ground state, $\beta_2^{\rm gs}$, obtained in three recent theoretical calculations of the ground state of even Ne isotopes, such as the deformed Hartree-Fock plus BCS calculations with Skyrme interaction [26], the deformed mean-field approach with BCS theory for pairing correlations [27], and the very recent relativistic Hartree-Fock-Bogoliubov model [28]. We note that these studies are found to reproduce quite accurately the experimental charge radii of Ne isotopes (determined by optical isotope shifts measurements [29]), across the *sd* neutron shell. As shown in the figure, the models predict that the deformation decreases close to the middle of the *sd* shell, as a consequence of the closure of the $d_{5/2}$ subshell [29], which favors a spherical state or a small oblate deformation for $I^\pi = 0^+$ and 2^+, while a prolate deformation is expected already at $I^\pi = 4^+$ [30]. Our data may suggest a similar trend, but a direct comparison is not possible, because the transition strengths are not calculated in these studies.

IV. CONCLUSION

In this paper we have studied the dynamics of the heavy-ion reaction ^{22}Ne + ^{208}Pb at 128 MeV beam energy. The experiment was performed at Legnaro National Laboratories, using the PRISMA-CLARA experimental setup, which allowed particle-γ coincidence measurements. Elastic, inelastic, and one-nucleon transfer differential cross sections were measured and compared with semiclassical and distorted-wave Born approximation calculations, resulting in a global agreement between data and theory. A key point of the analysis was the study of the angular distribution of the 2^+ state of ^{22}Ne by the DWBA model, together with similar calculations performed for the 2^+ state of the unstable ^{24}Ne nucleus, based on existing data from the ^{24}Ne + ^{208}Pb reaction at 182 MeV beam energy [10]. In both cases the DWBA model gives a good reproduction of the data and allows the determination of the β_2^C deformation parameter of the nuclear charge distribution. In particular, the analysis provides a very small β_2^C value for ^{24}Ne. This is consistent with the trend predicted for the evolution of ground state quadrupole deformation $\beta_2^{\rm gs}$ along the Ne isotopic chain, which suggests a subshell closure at $N = 14$. Such a result calls for additional experimental investigation on this nucleus, which is of key importance for the understanding of the shell structure along the Ne isotopic chain.

In conclusion, the present work demonstrates the validity of heavy-ion reaction studies for both dynamics and nuclear structure investigations, providing a fruitful method which could be further exploited in the future for the investigation of very exotic species. This will require the use of a high-efficiency γ-detector spectrometer, such as the AGATA array currently under development [31–33], coupled to a large acceptance spectrometer, such as PRISMA at Legnaro or VAMOS at GANIL.

ACKNOWLEDGMENTS

This work was supported by the Italian Istituto Nazionale di Fisica Nucleare and partially by the Spanish MICINN (AIC10-D-000568 bilateral action and FPA2008-06419) and Generalitat Valenciana (Grant PROMETEO/2010/101). The work was also partially supported by the Polish Ministry of Science and Higher Education (Grant No. N N202 309135).

[1] L. Corradi, G. Pollarolo, and S. Szilner, J. Phys. G **36**, 113101 (2009).
[2] R. Broda, J. Phys. G **32**, R151 (2006).
[3] J. J. Valiente-Dobon *et al.*, Phys. Rev. Lett. **102**, 242502 (2009).
[4] S. Bhattacharyya *et al.*, Phys. Rev. Lett. **101**, 032501 (2008).
[5] D. Montanari *et al.*, Phys. Rev. C **84**, 054613 (2011).
[6] D. Montanari *et al.*, Phys. Lett. B **697**, 288 (2011).
[7] D. Montanari *et al.*, Phys. Rev. C **85**, 044301 (2012).
[8] A. Winther, Nucl. Phys. A **594**, 203 (1995).
[9] M. Rhoades-Brown, M. H. Macfarlane, and S. C. Pieper, Phys. Rev. C **21**, 2417 (1980); **21**, 2436 (1980).
[10] G. Benzoni *et al.*, Eur. Phys. J. A **45**, 287 (2010).

[11] A. Gadea *et al.*, Eur. Phys. J. A **20**, 193 (2004).
[12] A. M. Stefanini *et al.*, Nucl. Phys. A **701**, 217c (2002).
[13] G. Montagnoli *et al.*, Nucl. Instr. Meth. A **547**, 455 (2005).
[14] S. Beghini *et al.*, Nucl. Instr. Meth. A **551**, 364 (2005).
[15] D. Montanari *et al.*, Eur. Phys. J. A **47**, 4 (2011).
[16] S. Szilner *et al.*, Phys. Rev. C **76**, 024604 (2007).
[17] R. A. Broglia and A. Winther, *Heavy Ion Reactions* (Addison-Wesley, Redwood City, CA, 1991).
[18] E. E. Gross *et al.*, Phys. Rev. C **29**, 459 (1984).
[19] W. D. Myers and K.-H. Schmidt, Nucl. Phys. A **410**, 61 (1983).
[20] National Nuclear Data Center, Brookhaven National Laboratory, http://www.nndc.bnl.gov/.
[21] L. A. Riley, P. D. Cottle, M. Fauerbach, T. Glasmacher, K. W. Kemper, B. V. Pritychenko, and H. Scheit, Phys. Rev. C **62**, 034306 (2000).
[22] H. Scheit *et al.*, Eur. Phys. J. A **25**, 397 (2005).
[23] J. Gibelin *et al.*, Phys. Rev. C **75**, 057306 (2007).
[24] H. Iwasaki *et al.*, Phys. Lett. B **620**, 118 (2005).
[25] B. A. Watson, J. A. Becker, and T. R. Fisher, Phys. Rev. C **9**, 1200 (1974).
[26] T. Siiskonen, P. O. Lipas, and J. Rikovska, Phys. Rev. C **60**, 034312 (1999).
[27] G. A. Lalazissis, A. R. Farhan, and M. M. Sharma, Nucl. Phys. A **628**, 221 (1998).
[28] J.-P. Ebran, E. Khan, D. Pena Arteaga, and D. Vretenar, Phys. Rev. C **83**, 064323 (2011).
[29] K. Marinova *et al.*, Phys. Rev. C **84**, 034313 (2011).
[30] R. R. Rodriguez-Guzman, J. L. Egido, and L. M. Robledo, Eur. Phys. J. A **17**, 37 (2003).
[31] D. Bazzacco, Nucl. Phys. A **746**, 248c (2004).
[32] A. Gadea *et al.*, Nucl. Instr. Meth. A **654**, 88 (2011).
[33] S. Akkoyun *et al.*, Nucl. Instr. Meth. A **668**, 26 (2012).